

Magnetic cryocooling with Gd^{3+} centers in a light and compact framework

G. Lorusso,¹ J. W. Sharples,² E. Palacios,¹ O. Roubeau,¹ E. K. Brechin,³ R. Sessoli,⁴ A. Rossin,⁵ F. Tuna,² E. J. L. McInnes,² D. Collison,² and M. Evangelisti^{1, a)}

¹⁾*Instituto de Ciencia de Materiales de Aragón (ICMA), CSIC – Universidad de Zaragoza, Departamento de Física de la Materia Condensada, 50009 Zaragoza, Spain*

²⁾*School of Chemistry and Photon Science Institute, The University of Manchester, M13-9PL Manchester, United Kingdom*

³⁾*School of Chemistry, The University of Edinburgh, EH9-3JJ Edinburgh, United Kingdom*

⁴⁾*Department of Chemistry and INSTM, Università degli Studi di Firenze, 50019 Sesto Fiorentino, Italy*

⁵⁾*Istituto di Chimica dei Composti Organometallici (ICCOM), CNR, 50019 Sesto Fiorentino, Italy*

(Dated: 24 October 2018)

The magnetocaloric effect of gadolinium formate, $Gd(OOCH)_3$, is experimentally determined down to sub-Kelvin temperatures by direct and indirect methods. This 3D metal-organic framework material is characterized by a relatively compact crystal lattice of weakly interacting Gd^{3+} spin centers interconnected via light formate ligands, overall providing a remarkably large magnetic:non-magnetic elemental weight ratio. The resulting volumetric magnetic entropy change is decidedly superior in $Gd(OOCH)_3$ than in the best known magnetic refrigerant materials for liquid-helium temperatures and low-moderate applied fields.

PACS numbers: 75.30.Sg; 75.40.Cx

^{a)}<http://molchip.unizar.es/>

Recent years have witnessed a terrific increase in the number of molecule-based materials proposed as magnetic refrigerants for liquid-helium temperatures.^{1–15} Refrigeration proceeds adiabatically via the magnetocaloric effect (MCE), which describes the changes of magnetic entropy (ΔS_m) and adiabatic temperature (ΔT_{ad}), following a change in the applied magnetic field (ΔB). As in the first paramagnetic salt that permitted sub-Kelvin temperatures to be reached in 1933,¹⁶ gadolinium is often present because its orbital angular momentum is zero and it has the largest entropy per single ion.¹ How to spatially assemble the Gd^{3+} spin centers is vital for designing the ideal magnetic refrigerant.^{9,15} On the one hand, the magnetic density should be maximized, for instance, by limiting the amount of non-magnetic elements which act passively in the physical process. On the other hand, the magnetic ordering for $B = 0$ should not develop, causing the decrease of MCE, above the target working temperature of the refrigerant. Therefore a compromise becomes necessary, especially for reaching very low temperatures.

This letter focuses on gadolinium formate, whose chemical formula reads $\text{Gd}(\text{OOCH})_3$, which belongs to the class of metal-organic framework (MOF) materials. Other three-dimensional MOF materials have recently attracted the interest for their cooling properties, combined with their synthetic variety and intrinsic robustness.^{10–15} We shall see below that, while presenting a sub-Kelvin ordering temperature, $\text{Gd}(\text{OOCH})_3$ is also characterized by a relatively high packing density of Gd^{3+} ions, linked only to light formate ligands. The resulting MCE, that we estimate by direct and indirect methods, sets $\text{Gd}(\text{OOCH})_3$ in an enviable position within this research area.

Single-crystal structure determination of $\text{Gd}(\text{OOCH})_3$ completes the original results derived from powder diffraction.^{17,18} No previous magnetic measurements on $\text{Gd}(\text{OOCH})_3$ are reported in the literature, except for initial Mössbauer experiments.¹⁹ Magnetization measurements down to 2 K and heat capacity measurements using the relaxation method down to ≈ 0.35 K were carried out on powder samples by means of commercial setups for $0 < B < 5$ T and $0 < B < 7$ T, respectively. Direct measurements of the MCE were performed on a powder sample using a dedicated thermal sensor, installed in the same setup employed for the heat capacity experiments.

Figure 1 shows the measured molar magnetization M for temperatures within 2 – 10 K. The magnetization saturates to the expected value of $7 \mu_B$ for a Gd^{3+} spin moment, according to which $s = 7/2$ and $g = 2$. The $M(T)$ curves can be well described by a Brillouin function

– see, e.g., the dashed line in Fig. 1 for an ideal paramagnet at $T = 2$ K. Deviations of the experimental data from the paramagnetic behavior are barely noticeable only for the lowest temperatures, and can be ascribed to the presence of a weak antiferromagnetic interaction. This is corroborated by the T -dependence of the magnetic susceptibility χ . As shown by the solid line in the inset of Fig. 1, the susceptibility data can be fitted above 2 K to a Curie-Weiss law $\chi = g^2 \mu_B^2 s(s + 1) / [3k_B(T - \theta)]$, obtaining a negative, though small, $\theta = -0.3$ K, which suggests that the Gd^{3+} moments are weakly antiferromagnetically correlated in the paramagnetic phase.

The top panel of Figure 2 shows the measured low-temperature heat capacity C , normalized to the gas constant R , as a function of temperature for several applied fields. A sharp lambda-like peak can be observed in the zero-field data for $T_{C1} \simeq 0.8$ K, denoting the presence of a phase transition, which is accompanied by a smooth and tiny feature at $T_{C2} \approx 0.4$ K. The magnetic origin of both anomalies is proved by the fact that external applied fields quickly and fully suppress them.²⁰ In agreement with $M(T, B)$, the analysis of the field-dependent C reveals that magnetic interactions between the Gd^{3+} spin centers are relatively weak, since applied fields $B \geq 1$ T are sufficient for fully decoupling all spins. As indeed shown in Fig. 2, the calculated Schottky contributions (solid lines) for the field-split

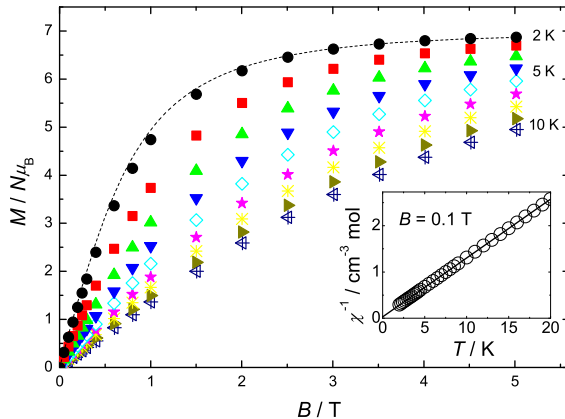


FIG. 1. Field-dependence of the experimental molar magnetization M for temperatures ranging from 2 to 10 K, with a 1 K step between adjacent isothermal curves. Dashed line is the calculated M of a paramagnet for $s = 7/2$, $g = 2$ and $T = 2$ K. Inset: temperature-dependence of the inverse of the experimental molar susceptibility χ collected for $B = 0.1$ T and Curie-Weiss fit (solid line).

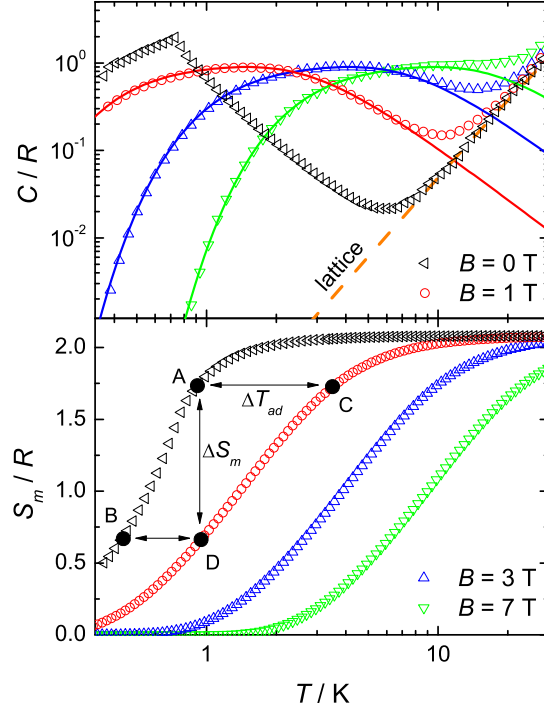


FIG. 2. Top: temperature-dependence of the heat capacity C normalized to the gas constant R collected for $B = 0, 1, 3$, and 7 T, as labeled. Solid thick lines are the calculated Schottky contributions for the corresponding B , and dashed line is the fitted lattice contribution. Bottom: T -dependence of the experimental magnetic entropy S_m normalized to the gas constant R for several B , as obtained from the magnetic contribution C_m to the total heat capacity. Highlighted examples of magnetic entropy change ΔS_m between states $A \leftrightarrow D$ and adiabatic temperature changes ΔT_{ad} between states $A \leftrightarrow C$ and $B \leftrightarrow D$.

levels of the non-interacting $s = 7/2$ multiplet nicely account for the magnetic contribution C_m to the experimental heat capacity. For $T \gtrsim 7$ K, a large field-independent contribution appears, which can be attributed to the lattice phonon modes of the crystal. The dashed line in the top panel of Fig. 2 represents a fit to this contribution, with the well-known Debye function yielding a value of $\Theta_D = 168$ K for the Debye temperature, which is remarkably large among molecular²¹ and MOF¹⁵ materials, denoting a relatively stiff lattice. A larger Θ_D implies a correspondingly lower lattice entropy in the low- T region, ultimately favoring the MCE. From the experimental heat capacity the temperature dependence of the magnetic

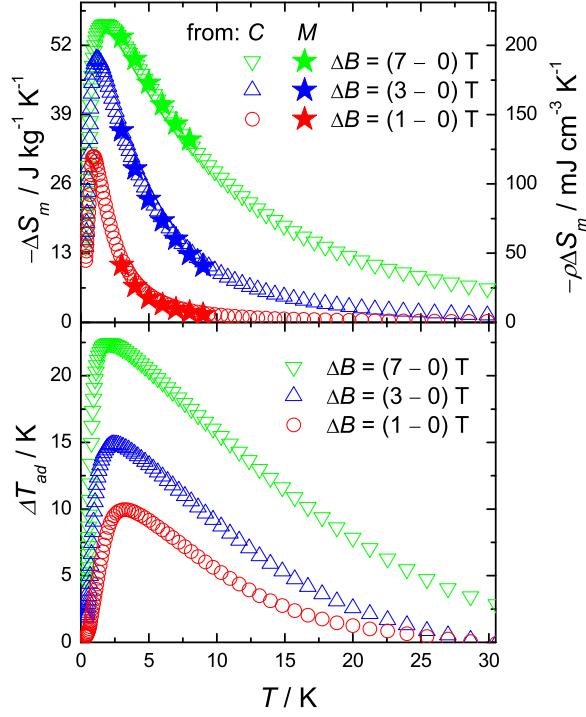


FIG. 3. Top: temperature-dependence of the magnetic entropy change ΔS_m , as obtained from magnetization and heat capacity data (Figs. 2 and 3, resp.) for the indicated applied-field changes ΔB . Vertical axis reports units in $\text{J kg}^{-1} \text{K}^{-1}$ (left) and volumetric $\text{mJ cm}^{-3} \text{K}^{-1}$ (right). Bottom: T -dependence of the adiabatic temperature change ΔT_{ad} , as obtained from heat capacity data for the indicated ΔB .

entropy $S_m(T)$ is derived by integration, i.e.,

$$S_m(T) = \int_0^T \frac{C_m(T)}{T} dT, \quad (1)$$

where C_m is obtained by subtracting the lattice contribution to the total C measured. The so-obtained $S_m(T)$ is shown in the bottom panel of Fig. 2 for the corresponding applied fields. For $B = 0$, the lack of experimental C_m for $T \lesssim 0.3$ K has been taken into account by matching the limiting S_m at high T with the value obtained from the in-field data. One can notice that there is a full entropy content of $R \ln(8)$ per mole Gd^{3+} involved, as expected from $R \ln(2s + 1)$ and $s = 7/2$.

Next, we *indirectly* evaluate the MCE of $\text{Gd}(\text{OOCH})_3$ from the experimental data pre-

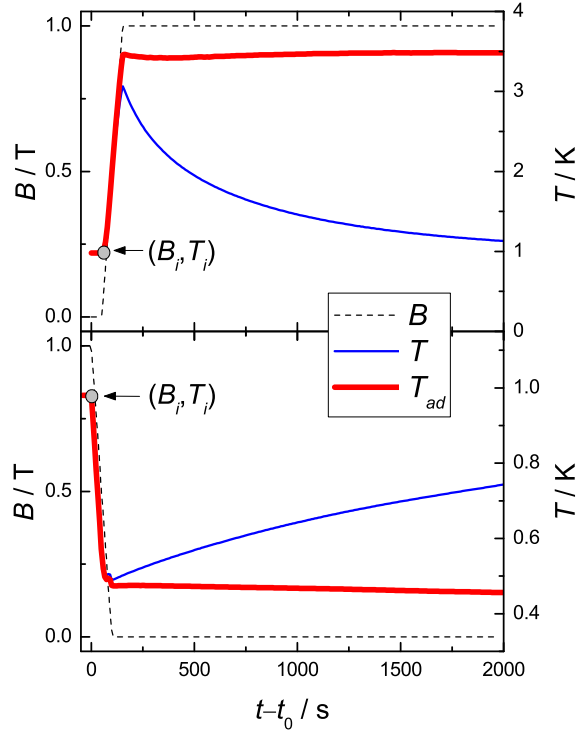


FIG. 4. Time evolution of the applied field B , experimental temperature T and deduced adiabatic temperature T_{ad} , as labeled, during a magnetization (top) and a demagnetization (bottom) process, both starting from B_i and $T_i = 0.95$ K.

sented so far. From the bottom panel of Fig. 2, we straightforwardly obtain the magnetic entropy changes $\Delta S_m(T, \Delta B)$ for different applied field changes $\Delta B = B_f - B_i$. The so-obtained results are depicted in Figure 3. A similar set of data can also be derived from an isothermal process of magnetization by employing the Maxwell relation, i.e., $\Delta S_m(T, \Delta B) = \int_{B_i}^{B_f} [\partial M(T, B) / \partial T]_B dB$. From the experimental $M(T, B)$ data in Fig. 1, we then obtain curves that rather beautifully corroborate the corresponding results previously derived from heat capacity – see top panel of Fig. 3. Furthermore, to a cooling process under adiabatic conditions, one naturally associates a temperature change whose estimate is made feasible by knowing C and thus S_m . The bottom panel of Fig. 3 shows $\Delta T_{ad}(T, \Delta B)$, where T denotes the final temperature of the adiabatic cooling, e.g., for going from states C ($T = 3.4$ K, $B = 1$ T) to A ($T = 0.95$ K, $B = 0$) in Fig. 2.

A far more elegant and reliable method for determining the MCE is by *directly* measuring $\Delta T_{ad}(T, \Delta B)$ under quasi-adiabatic conditions. The procedure comprises a full magnetization-demagnetization cycle, during which the experimental T and B are continuously recorded. In a half cycle, starting with the sample at an initial T_i , we magnetize (demagnetize) by gradually increasing (decreasing) the applied field from B_i to B_f and let the sample relax to the final T_f . In order to compute the temperature evolution for an *ideal* adiabatic process, one requires a precise knowledge of the heat that unavoidably is absorbed from (released to) the thermal bath during the direct measurement. For this purpose, the thermal conductance k of the wires holding our sensor was previously determined as a function of T , using a standard copper piece as the sample. The non-adiabaticity induces a variation of the entropy $\Delta S = S(t) - S(t_0)$ in a time interval $t - t_0$, which can be expressed as $\Delta S = \int_{t_0}^t k(T_i - T)/T dt$ at every time instant. Besides, from Eq. 1 we also have $\Delta S = \int_{T_{ad}}^T C(T, B)/T dT$, where the adiabatic temperature T_{ad} , viz., the temperature if the sample would have been kept thermally isolated, is the only unknown and can therefore be deduced numerically. In our treatment, we safely disregard the entropy contribution due to the heat transferred from the sample holder to the refrigerant material, i.e., $\Delta S_{sh} = \int_{T_i}^{T_f} C_{sh}/T dT$, since the heat capacity of the sample holder C_{sh} is negligible with respect to that of $\text{Gd}(\text{OOCH})_3$ below liquid-helium temperature.

Figure 4 shows the time evolution of B , T and T_{ad} for a full magnetization-demagnetization cycle, starting at $T_i = 0.95$ K and for a field change $\Delta B = B_f - B_i = (1 - 0)$ T or $(0 - 1)$ T, depending on whether we deal with the magnetization or demagnetization process, respectively. We note that the exact same conditions are highlighted in Figure 2: process A \rightarrow C for the magnetization and process D \rightarrow B for the demagnetization. In the top panel of Fig. 4, we observe T to increase while we magnetize to 1 T. Here T_{ad} increases more than T because the thermal losses to the bath are compensated to obtain T_{ad} . Upon reaching B_f , T decays back towards $T_i = 0.95$ K but $T_{ad} = 3.5$ K is constant, since it corresponds to an adiabatic process at constant B . In the bottom panel, T decreases below T_i , while we demagnetize to zero field, whereupon T gradually relaxes back to equilibrium, while constant $T_{ad} = 0.45$ K. Remarkably, the final adiabatic temperatures of 3.5 K and 0.45 K obtained after sweeping the field up and down, respectively, corroborate the results independently inferred by an indirect method – see states C and B, respectively, in Figure 2.

The MCE of $\text{Gd}(\text{OOCH})_3$ is exceptionally large, especially in comparison with other

molecule-based magnetic refrigerants. A fine example is the recently studied dimeric light molecule $[\{\text{Gd}(\text{OAc})_3(\text{H}_2\text{O})_2\}_2] \cdot 4\text{H}_2\text{O}$, hereafter shortened as $\{\text{Gd}_2\}$, whose $-\Delta S_m$ reaches a value as large as $40.6 \text{ J kg}^{-1} \text{ K}^{-1}$ for $\Delta B = (7 - 0) \text{ T}$ and $T \simeq 1.8 \text{ K}$.⁸ For widespread applications, the interest is chiefly restricted to applied fields which can be produced with permanent magnets, viz., in the range $1 - 2 \text{ T}$. In this regard $\{\text{Gd}_2\}$ could be appealing because a weak, ferromagnetic intracluster exchange interaction enhances the MCE for low applied fields, yielding an outstanding $-\Delta S_m = 27.0 \text{ J kg}^{-1} \text{ K}^{-1}$ for $\Delta B = (1 - 0) \text{ T}$ and $T \simeq 0.8 \text{ K}$. However, these values are not as large as the ones we here report for $\text{Gd}(\text{OOCH})_3$, e.g., $-\Delta S_m = 56.0 \text{ J kg}^{-1} \text{ K}^{-1}$ and $31.2 \text{ J kg}^{-1} \text{ K}^{-1}$ for $\Delta B = (7 - 0) \text{ T}$ and $(1 - 0) \text{ T}$, respectively, at similar corresponding temperatures such as seen in Figure 3.

Gadolinium gallium garnet (GGG) is *the* reference magnetic refrigerant material for the liquid-helium temperature region.^{22,23} Indeed, its functionality is commercially exploited in spite of a relatively modest maximum $-\Delta S_m = 20.5 \text{ J kg}^{-1} \text{ K}^{-1}$ for $\Delta B = (2 - 0) \text{ T}$. This apparent contradiction is resolved by measuring the entropy change in terms of equivalent volumetric units, which take into consideration the GGG mass density $\rho = 7.08 \text{ g cm}^{-3}$. By so-doing, GGG achieves a record value $-\rho\Delta S_m \simeq 145 \text{ mJ cm}^{-3} \text{ K}^{-1}$ for the same applied field change of 2 T . Although these units are not often used to characterize the MCE, they are better suited for assessing the implementation of the refrigerant material in a designed apparatus.²⁴ On this point, one could correctly argue that the MCE of molecule-based refrigerant materials is disfavored by their typically low ρ . For instance, $\rho = 2.04 \text{ g cm}^{-3}$ for the aforementioned $\{\text{Gd}_2\}$, which results in $-\rho\Delta S_m \simeq 56 \text{ mJ cm}^{-3} \text{ K}^{-1}$ and $73 \text{ mJ cm}^{-3} \text{ K}^{-1}$ for $\Delta B = (1 - 0) \text{ T}$ and $(3 - 0) \text{ T}$, respectively,⁸ i.e., definitely much lower than GGG.

The mass density $\rho = 3.86 \text{ g cm}^{-3}$ of $\text{Gd}(\text{OOCH})_3$ is very large among molecule-based materials, though yet smaller than that of GGG. In $\text{Gd}(\text{OOCH})_3$, the Gd^{3+} centers are interconnected only by short and extremely light CHOO^- ligands. Ultimately, this enhances the MCE favored by a larger weight of magnetic elements with respect to non-magnetic ones, which act passively. As a matter of fact, the mass density of these two materials is effectively counterbalanced by the magnetic:non-magnetic weight ratio, which amounts to 0.54 in $\text{Gd}(\text{OOCH})_3$ and to a lower 0.47 in GGG.²⁵ For comparison, this number further reduces to 0.39 in the case of $\{\text{Gd}_2\}$. Overall, adopting the proper units, the MCE of $\text{Gd}(\text{OOCH})_3$ is characterized by maxima $-\rho\Delta S_m \simeq 120 \text{ mJ cm}^{-3} \text{ K}^{-1}$ and $189 \text{ mJ cm}^{-3} \text{ K}^{-1}$ for $\Delta B = (1 - 0) \text{ T}$ and $(3 - 0) \text{ T}$, respectively, as can be seen in Figure 3. These values

compares favorably with the ones obtained from GGG.

Concluding, we experimentally determine the magnetocaloric effect of the $\text{Gd}(\text{OOCH})_3$ metal-organic framework material. Under quasi-adiabatic conditions, sub-Kelvin direct measurements of the temperature change corroborate the results inferred from indirect methods. By comparing the MCE per volume of other known materials, such as GGG, we demonstrate that gadolinium formate could serve as an excellent magnetic refrigerant for liquid helium temperatures. Our observations are interpreted as the result of a light and compact structural framework promoting very weak magnetic correlations between the Gd^{3+} spin centers. Finally, we foresee that synthetic and technological strategies, already developed for the surface deposition of MOF materials, could ultimately facilitate the integration and exploitation of $\text{Gd}(\text{OOCH})_3$ within molecule-based microdevices for on-chip local refrigeration.²⁶

ACKNOWLEDGMENTS

We thank E. Moreno Pineda. This work has been supported by the Spanish MINECO through grant MAT2012-38318, and by an EU Marie Curie IEF (to G. L.).

REFERENCES

- ¹For a recent review see, e.g., M. Evangelisti and E. K. Brechin, *Dalton Trans.* **39**, 4672 (2010), and references therein.
- ²See, e.g., R. Sessoli, *Angew. Chem. Int.-Ed.* **51**, 43 (2012).
- ³F. Torres, J. M. Hernández, X. Bohigas and J. Tejada, *Appl. Phys. Lett.* **77**, 3248 (2000).
- ⁴Yu. I. Spichkin, A. K. Zvezdin, S. P. Gubin, A. S. Mischenko and A. M. Tishin, *J. Phys. D: Appl. Phys.* **34**, 1162 (2001).
- ⁵M. Affronte, A. Ghirri, S. Carretta, G. Amoretti, S. Piligkos, G. A. Timco and R. E. P. Winpenny, *Appl. Phys. Lett.* **84**, 3468 (2004).
- ⁶M. Evangelisti, A. Candini, A. Ghirri, M. Affronte, E. K. Brechin and E. J. L. McInnes, *Appl. Phys. Lett.* **87**, 072504 (2005).
- ⁷M. Evangelisti, A. Candini, M. Affronte, E. Pasca, L. J. de Jongh, R. T. W. Scott and E. K. Brechin, *Phys. Rev. B* **79**, 104414 (2009).

- ⁸M. Evangelisti, O. Roubeau, E. Palacios, A. Camón, T. N. Hooper, E. K. Brechin and J. J. Alonso, *Angew. Chem. Int.-Ed.* **50**, 6606 (2011).
- ⁹M.-J. Martínez-Pérez, O. Montero, M. Evangelisti, F. Luis, J. Sesé, S. Cardona-Serra and E. Coronado, *Adv. Mater.* **24**, 4301 (2012).
- ¹⁰E. Manuel, M. Evangelisti, M. Affronte, M. Okubo, C. Train and M. Verdaguer, *Phys. Rev. B* **73**, 172406 (2006).
- ¹¹M. Evangelisti, E. Manuel, M. Affronte, M. Okubo, C. Train and M. Verdaguer, *J. Magn. Magn. Mater.* **316**, e569 (2007).
- ¹²L. Sedláková, J. Hanko, A. Orendčov, M. Orendáč, C. L. Zhou, W. H. Zhu, B. W. Wang, Z. M. Wang and S. Gao, *J. Alloys Compd.* **487**, 425 (2009).
- ¹³R. Sibille, T. Mazet, B. Malaman and M. François, *Chem. Eur. J.* **18**, 12970 (2012).
- ¹⁴F.-S. Guo, Y.-C. Chen, J.-L. Liu, J.-D. Leng, Z.-S. Meng, P. Vrábek, M. Orendáč and M.-L. Tong, *Chem. Commun.* **48**, 12219 (2012).
- ¹⁵G. Lorusso, M. A. Palacios, G. S. Nichol, E. K. Brechin, O. Roubeau and M. Evangelisti, *Chem. Commun.* **48**, 7592 (2012).
- ¹⁶W. F. Giaque and D. P. MacDougall, *Phys. Rev. B* **43**, 768 (1933).
- ¹⁷A. Pabst, *J. Chem. Phys.* **11**, 145 (1943).
- ¹⁸Gd(OOCH)₃ crystallizes in space group $R3m$ with $a = b = 10.4583(4)$ Å, $c = 3.9869(3)$ Å, $\alpha = \beta = 90^\circ$, $\gamma = 120^\circ$ and $Z = 3$. The distance between nearest and next-nearest Gd neighbors is 3.98 Å and 6.19 Å, respectively. CCDC-914467 contains the supplementary crystallographic data, which can be obtained free of charge via www.ccdc.cam.ac.uk/conts/retrieving.html.
- ¹⁹J. D. Cashion, D. B. Prowse and A. Vas, *J. Phys. C: Solid State Phys.* **6**, 2611 (1973).
- ²⁰We refrain from discussing the magnetic ordering mechanism any further since this topic exceeds the scope of this article and its full comprehension requires additional measurements, whose results will be exhaustively presented elsewhere.
- ²¹See, e.g., M. Evangelisti, F. Luis, L. J. de Jongh and M. Affronte, *J. Mater. Chem.* **16**, 2534 (2006), and references therein.
- ²²B. Daudin, R. Lagnier and B. Salce, *J. Magn. Magn. Mater.* **27**, 315 (1982).
- ²³T. Numazawa, K. Kamiya, T. Okano and K. Matsumoto, *Physica B* **329-333**, 1656 (2003).
- ²⁴See, e.g., K. A. Gschneidner Jr., V. K. Pecharsky and A. O. Tsokol, *Rep. Prog. Phys.* **68**, 1479 (2005).

²⁵For $\text{Gd}(\text{OOCH})_3$, the relative molecular mass and number of Gd^{3+} ions per formula unit are $m = 292.30 \text{ g mol}^{-1}$ and $n = 1$, respectively. For GGG, $m = 1012.37 \text{ g mol}^{-1}$ and $n = 3$. For $\{\text{Gd}_2\}$, $m = 812.89 \text{ g mol}^{-1}$ and $n = 2$. Therefore, $nA_r/m = 0.54, 0.47$ and 0.39 for $\text{Gd}(\text{OOCH})_3$, GGG and $\{\text{Gd}_2\}$, respectively, where $A_r = 157.25 \text{ g mol}^{-1}$ is the gadolinium relative atomic mass.

²⁶G. Lorusso, M. Jenkins, P. González-Monje, A. Arauzo, J. Sesé, D. Ruiz-Molina, O. Roubeau and M. Evangelisti, arXiv:1212.1880.